Toy Monte Carlo of Neutrino Beam Production for T2K Experiment

Sourav Sarkar

April 11, 2018

Email: ssarkar1@ualberta.ca
Student ID: 1512784

1 Introduction

Neutrinos are one of the fundamental particles in the standard model of particle physics. They interact with other particles only through weak interactions. Due to very small interaction cross section, neutrinos travel long distances before they interact. Particle physicists exploit this along with the fact that neutrinos are abundant almost everywhere in the universe, to study neutrinos for various aspects. Neutrinos coming from the sun (called solar neutrinos) carry information about the structure of the sun. Neutrinos can also come from the core of the earth (geo neutrinos), from the cosmic ray interaction in the atmosphere (atmospheric neutrinos), other astrophysical objects (astrophysical neutrinos) etc. So the study of neutrino physics has the ability to answer many open questions in physics.
There are three neutrinos for the three generation of standard model fermions - electron neutrino (ν_e), muon neutrino (ν_μ) and tau neutrino (ν_τ). As neutrinos have very tiny masses, one neutrino flavor has the ability to oscillate into other neutrino flavor during its propagation through space. T2K experiment in Japan [1], is dedicated to study such neutrino oscillations. For this purpose, T2K generates an artificial beam of muon neutrinos from the accelerator facility at J-PARC [1] and let those neutrinos travel through matter before detecting them. By studying the deficit of muon neutrinos at the detector compared to the expectation, T2K measures the parameters involved in neutrino oscillation.
In this project, we aim to build a toy model of the accelerator system to simulate neutrino beam that are produced in T2K experiment. In section 2 of this report, we discuss all the principle physics processes involved for building the toy model. In the next section, we discuss the details of the model. All the limitations we have in our model is discussed in Section 4 and finally we present our simulation result in section 5.

2 Physics behind the Monte Carlo

T2K experiment is an accelerator based neutrino experiment to study the neutrino flavor oscillations. In this experiment a neutrino beam (primary composition is muon neutrinos ν_μ) is produced at the J-PARC accelerator facility and is directed to the Super-Kamiokande (SK) neutrino detector which is located 295Km away for oscillation studies. Apart from the SK detector, T2K uses additional detector ND280 [1] installed near the accelerator to study and monitor the flux quality of the neutrino beam. Neutrino beam is produced from the collision of accelerated protons on Aluminum target. We discuss the details of neutrino production in the following subsections.

2.1 Neutrino production processes

When high energy proton beam collides with nuclear targets it produces secondary particles through hadronic shower. These secondaries then leave the target with a boost in the forward direction. Among these secondaries, charged pions($\pi^{\pm}$) and kaons($K^{\pm}, K_L$) decay in flight through the following decay processes,

$$\begin{aligned} \pi^{\pm} &\longrightarrow \mu\nu_{\mu} \quad (BR \sim 100\%) \\ K^{\pm} &\longrightarrow \mu\nu_{\mu} \quad (BR \sim 63.4\%) \\ K_L &\longrightarrow \pi\mu\nu_{\mu} \quad (BR \sim 27.2\%). \end{aligned} \tag{1}$$

Decay products of these charged mesons are the primary source for the neutrinos at T2K. A small amount of background electron neutrinos (ν_e) is also generated from the decay of muons,

$$\mu \longrightarrow e\nu_{\mu}\nu_{e}. \tag{2}$$

At the J-PARC facility, accelerated pulsed proton beam of energy 12 GeV is collided on Aluminum target. Each pulse contains 3.3×10^{14} protons on target (POT) [2]. Secondary pions and kaons are produced through the hadron-nuclear interaction,

$$\begin{aligned} p + N &\longrightarrow \pi^{\pm} + X \\ p + N &\longrightarrow K^{\pm}/K_L + X \end{aligned} \tag{3}$$

We have mentioned before, due to the forward boost, produced secondary particles travel mostly along the beam axis. However from Fig. 1 we notice, there is a broad distribution of π^{+} (produced from the hadronic interactions) transverse momentum (p_T) which indicates that secondary particles travel with some divergence relative to the beam axis. Therefore the neutrinos produced from these secondaries will also have significant divergence. As neutrinos are neutral in charge and interact weakly, we cannot control their direction. To generate neutrino beam close to the beam axis we need to reduce the divergence of charged pions/kaons so that their decay products have as low divergence as possible.

2.2 Horn Magnets

T2K uses two magnetic horns [4] which controls the direction of charged pions and kaons by focusing them along the beam axis. Each magnetic horn consists of two coaxial cylindrical conductor sheets that are symmetric along the beam axis as shown in Fig. 2. When current sheet runs into the inner conductor and comes out from the outer conductor, the setup generates toroidal magnetic field in the region between the two conductors. Region outside the two conductors has zero magnetic field. The direction of the magnetic field is shown in the figure and the magnitude of the field is given as [5],

$$B = \frac{\mu_0 I}{2\pi r} \tag{4}$$

where μ_0 is the permeability of vacuum, I is the current in Amp which flows through the conductors, r is the radial distance. When a particle with charge q enters the magnetic field region, the Lorentz acting on the particle is,

$$\vec{F} = q\vec{v} \times \vec{B} \tag{5}$$

where $\vec{v}$ is the velocity of the particle. If we notice closely in Fig. 2, the inner conductor has the conical surface rather than cylindrical which is more useful in focusing pions and kaons with larger transverse momentum range. Also note that, these magnets focus particle with either

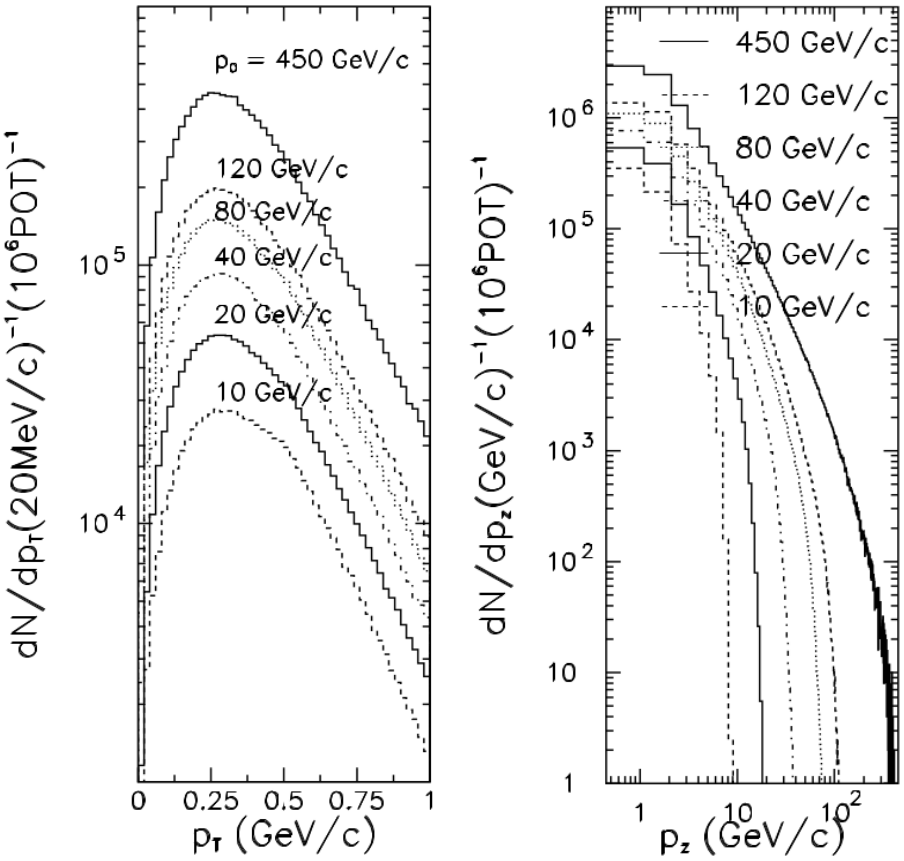

Figure 1: [Left]: Transverse momentum distribution of π^+ and [Right]: Longitudinal momentum distribution of pions at different energies[3].

positive charge or negative charge (not both) depending on the direction of the current flow in the conductors. According to the current flow direction shown in Fig. 2, all positive pions and kaons will be focused along the beam axis and all negative pions and kaons will be deflected outwards relative to the beam axis.

In T2K experiment, both magnetic horns have the highest peak current of 250 kA [5] (this value is optimized considering all the physical effects). Similar to proton beam, current flowing through these magnets is also pulsed and synchronized as shown in Fig. 3. Therefore all the spread-out positive pions and kaons produced in the collision will be deflected to be parallel to the beam axis when they travel through these two magnets and we get fairly focused pion/kaon beam.

2.3 Kinematics of neutrino beam

With the focused pion/kaon beam, let us now discuss the decay kinematics of these particles to understand the properties of neutrino beam. From Eq. 1, we see that first two decay processes follow two-body decay and third process follow three-body decay. Our discussion in this report is limited to only two-body decay case as three-body decay is not implemented in the toy Monte Carlo. Let us take the $\pi^{\pm} \longrightarrow \mu\nu_{\mu}$ process as example to show the necessary calculations.

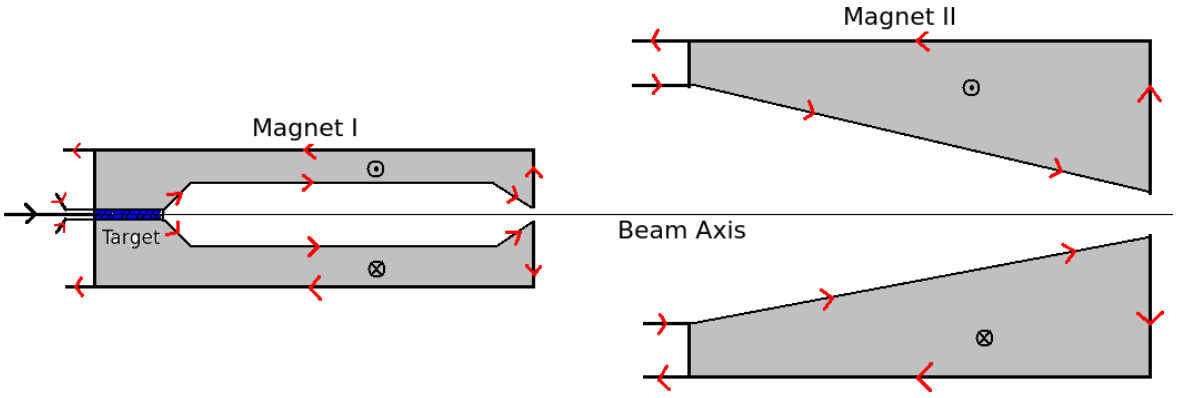

Figure 2: Schematic cross sectional view of the horn magnets at T2K. The blue region is the target, black arrow shows the direction of the proton beam. Red arrows indicate the direction of current flow in the magnets. Grey region is the active field region where the direction of the magnetic field is shown. Geometry details is taken from [6].

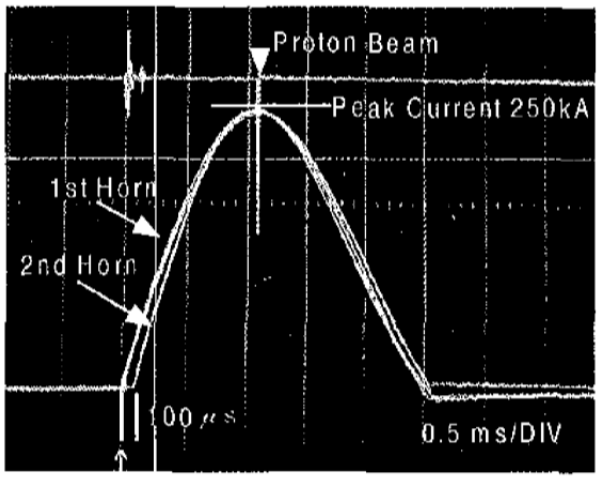

Figure 3: Current pulse shape in the horn magnet and synchronization with the proton beam pulse. [5]

In the center of mass (CM) frame of π, the energy-momentum conservation laws are as follows,

$$\begin{aligned} E_\mu + E_\nu &= m_\pi \\ p_\mu + p_\nu &= 0. \end{aligned} \tag{6}$$

From the conservation laws and taking neutrino mass $m_\nu \sim 0$, we get the neutrino energy in the CM frame as,

$$E_{CM} = \frac{m_\pi^2 - m_\mu^2}{2m_\pi} \approx 29.8MeV \tag{7}$$

So neutrinos have fixed energy in CM frame for the two body decays. Considering azimuthal symmetry, we consider two coordinate system in which the CM frame neutrino energy-momentum vector is expressed as,

$$P_{CM} = E_{CM}(1, sin\theta_{CM}, cos\theta_{CM}) \tag{8}$$

where θ_{CM} is the angle in the CM frame which follows isotropic distribution in 2-D plane (as the decay is spin independent).
Now if we apply Lorentz transformation along the direction of decaying pion, the energy-momentum vector components of neutrino in the lab frame along the pion direction is

$$\begin{aligned} E &= \gamma E_{CM}(1 + \beta cos\theta_{CM}) \\ Ecos\theta &= \gamma E_{CM}(cos\theta_{CM} + \beta) \\ Esin\theta &= E_{CM} sin\theta_{CM} \end{aligned} \tag{9}$$

where $\gamma = E_\pi/m_\pi$ and $\beta = p_\pi/E_\pi$. From the above equation we can set the kinematic limits on the energy and angle of the neutrino as,

$$\begin{aligned} \theta = sin^{-1}(\frac{E_{CM}}{E}) \leq \frac{E_{CM}}{E} \quad (forsmallangle) \\ \theta_{max} \approx \frac{29.8MeV}{E} \\ E_{max} \approx \frac{29.8MeV}{\theta}. \end{aligned} \tag{10}$$

As the angle $\theta = \theta(\gamma)$, for increasing pion energy E_π (i.e. increasing γ), maximum allowed angle θ_{max} will decrease leading to higher neutrino energy E. From the relations in Eq. 9, one can show that,

$$\frac{\partial E}{\partial \gamma} = \frac{E(cos\theta - \beta)}{\beta\gamma(1 - \beta cos\theta)} \tag{11}$$

So we see that the neutrino energy $E = E_{max}$ when $\beta = cos\theta$. So for a fixed angle θ, most of the neutrinos will be emitted at the pion energy for which $\beta = cos\theta$. However for higher pion energy, neutrinos have to be emitted more in the backward direction to maintain the fixed angle which results in decreasing neutrino energy. This effect can be seen in Fig. 4.

Finally, for a given pion energy distribution $g(E_\pi)$, we can calculate the analytical form of neutrino flux as function of energy E and angle θ as [7],

$$\frac{\partial^2 N}{\partial E \partial \Omega} = \frac{m_\pi}{4\pi E_{CM} sin^2\theta \sqrt{1 - (E/E_{CM})^2 sin^2\theta}} \times \left[g(E_\pi) | cos\theta \pm \sqrt{1 - (E/E_{CM})^2 sin^2\theta} | \right] \tag{12}$$

where '+' and '-' in the above equation depends on the condition $cos\theta > \beta$ and $cos\theta < \beta$ respectively.
Let us now discuss the details of the Monte Carlo where above physics model has been implemented.

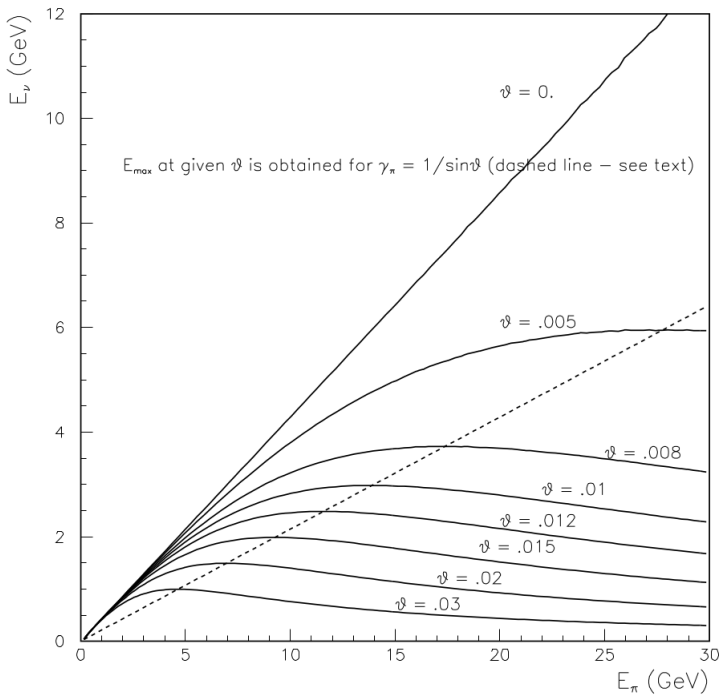

Figure 4: Maximum bound on the neutrino energy as a function of pion energy at different θ[7].

3 Model of the simulation

To simulate spectrum of the neutrino beam at T2K, we start with the simulation of proton beam - Aluminum target collision to produce pion/kaon secondaries. We then allow those pions/kaons to propagate through the horn magnets configuration and decay in flight to produce neutrinos according the physics discussed in the last section.

3.1 Hadron shower simulation

Simulation of proton beam colliding on the Aluminum target requires extensive treatment of hadron-nucleus interaction model which is beyond the scope of this project. For this reason, we have used FLUKA [8] to simulate hadron showers from proton nucleus interaction. FLUKA is a particle physics simulation package which is used for particle transportation and interactions in various medium.

In our FLUKA simulation, we have set the 12 GeV proton beam along Z-axis and interaction point at the origin (0,0,0) of the coordinate system. The geometry of the target is used as described in the T2K experiment [6] i.e. cylindrical rod. After the hadron shower simulation, we collect all the secondaries that leaves from the surface of the target medium. We have stored position, direction, energy and age of each secondaries as FLUKA simulation output. The collection of secondaries are then passed to the next stage of the simulation. Details of the FLUKA simulation input settings are summarized in Table 1. Also the input code for FLUKA run can be found in the appendix.

To validate the shower simulation in FLUKA we have plotted the transverse and longitudinal momentum distribution of pions and kaons from the collected secondaries. From Fig. 5, we see that the momentum distributions agree with the expectation as compared to Fig. 1. Now that we have validated the shower simulation, we can study the properties of the secondary pions. Fig. 6 shows the angular distribution of generated pions/kaons. From the figure we see that the distribution is peaked at around 20^0 instead of having maximum along the Z axis (i.e. $\theta = 0^0$), which indicates that the pion/kaon beam is indeed diverging away from the beam

Table 1: Details of the proton-Aluminum collision settings [6]

Paramter	Value
No. of Protons on Target (POT)	4×10^5
Beam Axis	Z
Primary interaction point	Origin (0,0,0)
Diameter of Target	20. mm
Length of Target	650. mm
Target Material	Aluminum (Al)

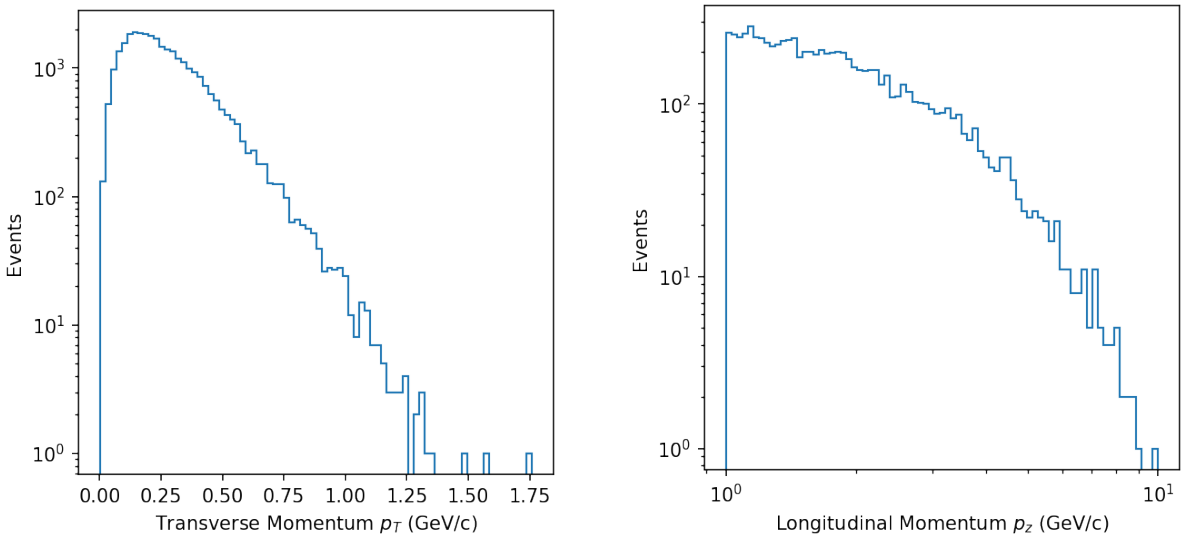

Figure 5: Transverse and longitudinal momentum of pions and kaons from 12 GeV proton collision on Al target.

axis. Also note that there are events with angle larger than 90^0 which denotes the backward going pions/kaons. Fig. 7 also shows the energy-angle correlation plot of the pions/kaons, from which we can interpret that most of pions are generated in the low energy regime and the distribution falls rapidly as we go in higher pion/kaon energies. As expected, higher energy pions are accumulated only at the small θ i.e. along the beam axis.
In the next section, let us now discuss the simulation of horn magnets which will focus the pion/kaon beam along the beam axis.

3.2 Horn magnet simulation

Two horn magnets in T2K experiment are optimized in volume, geometry, magnetic field strength and material to maximize the nuetrino flux as much as possible. The cross sectional diagram of the magnets is shown in Fig. 2. To increase the acceptance of diverging pions, the target medium is incorporated in the inner conductor of the first horn magnet (also shown in Fig. 2). Both the inner and outer conductor of the magnets are made of Aluminum alloy [6]. Geometrical details of the magnets are given in Table 2.

To simulate the magnetic field, we first define the magnet boundaries based on the geometry details in Table 2. The boundaries enclose the active field region between inner and outer conductors. Then we define the magnetic field direction and magnitude based on Eq. 4 on any point which falls in the active region. Any point outside the active region, we set the magnetic field to be simply zero.

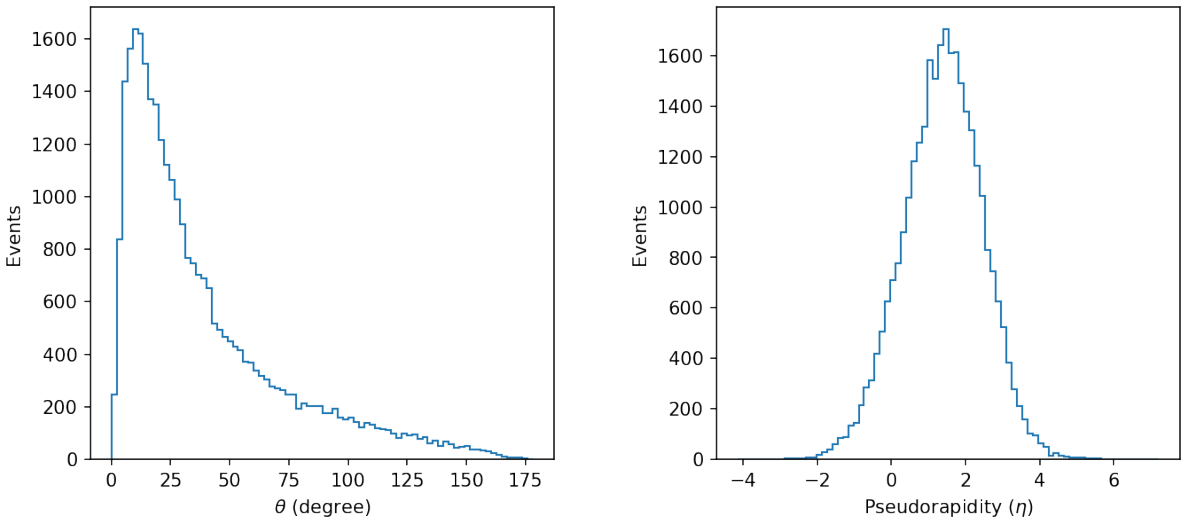

Figure 6: Angular and pseudorapidity distribution of the pions/kaons in our model.

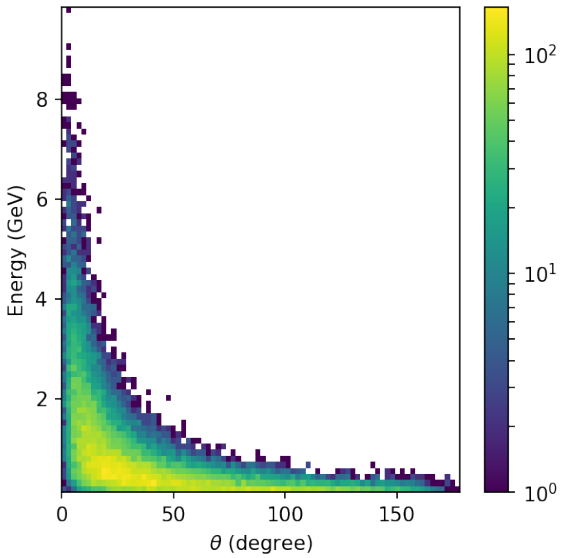

Figure 7: Energy-Angle correlation distribution of pions/kaons.

Table 2: Details of the horn magnets [6].

Parameters	**Magnet I**	**Magnet II**
Total length	2371 mm	2760 mm
Max. Diameter of inner conductor	136 mm	600 mm
Min. Diameter of inner conductor	20 mm	100 mm
Diameter of outer conductor	620 mm	1520 mm
Distance between two magnets	8060 mm	

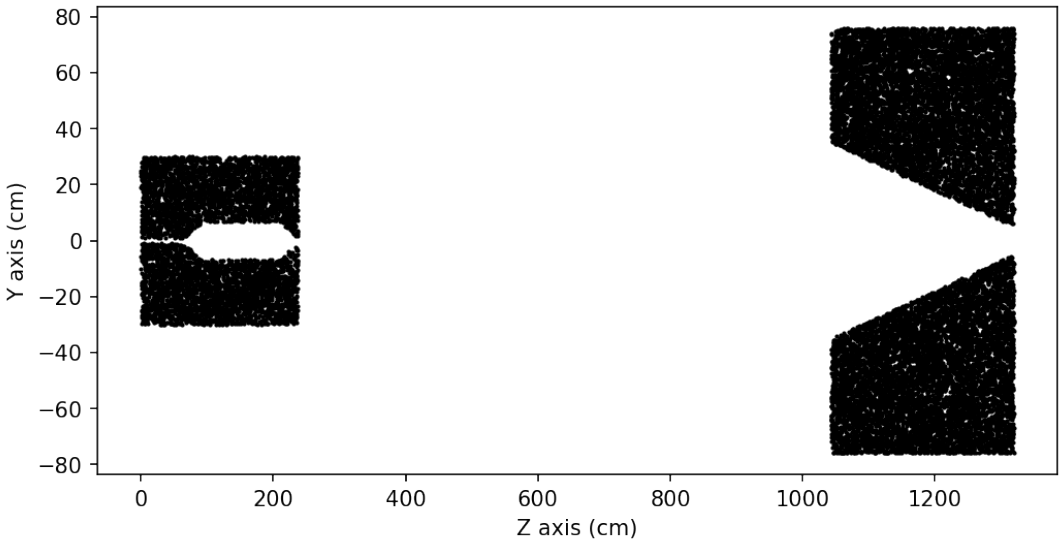

Figure 8: Scatter plot of the random positions inside the active field region.

To validate the implementation of magnet geometry, we throw many random positions in space covering both the magnets and select only those positions which fall in the active region. Fig. 8 shows the active region positions in the Y-Z plane, from which we successfully retrieve the cross sectional view of our magnets.

In the next section, we will now discuss the propagation of pions/kaons through the defined geometry and simulate their in flight decay.

3.3 Propagation and decay of pions/kaons

In this toy simulation, we will only consider the first two processes in Eq. 1, so we have only implemented the two body decay kinematics as discussed in section 2. In the simulation we collect all the charged pions and kaons from the FLUKA output and set their position, direction and energy as the initial condition for the numerical integration (using `odeint`) of equation of motion which follows the simple expressions,

$$\begin{aligned} \frac{d\vec{x}}{dt} &= \vec{v} \\ \frac{d\vec{v}}{dt} &= q\vec{v} \times \vec{B} \quad \text{Inside field active region} \\ &= 0 \quad \text{Outside field active region} \end{aligned} \tag{13}$$

In our propagation of particles, we have assumed the medium to be vacuum (i.e. no energy loss in flight) and also have ignored the absorption and scattering of pions/kaons at the magnet boundaries. As we are simulating events with order of 10^7 times smaller compared to the T2K events in each pulse, loosing events due to absorption and scattering would be statistically expensive for our small dataset.
With the implementation of particle propagation, we can now validate the effect of magnetic field defined in the `Magnet Class` of our code. Fig. 9 shows the effect of magnetic field on the diverging pion/kaon secondaries (taking a small fraction of the actual dataset). The plot shows the X-Y projection of all pion and kaon positions after propagating a fixed amount of time (100 ns). We notice that most of the particles have been accumulated either in the center (along the beam axis) or in the outer ring. As we have discussed before, with T2K magnet configuration all

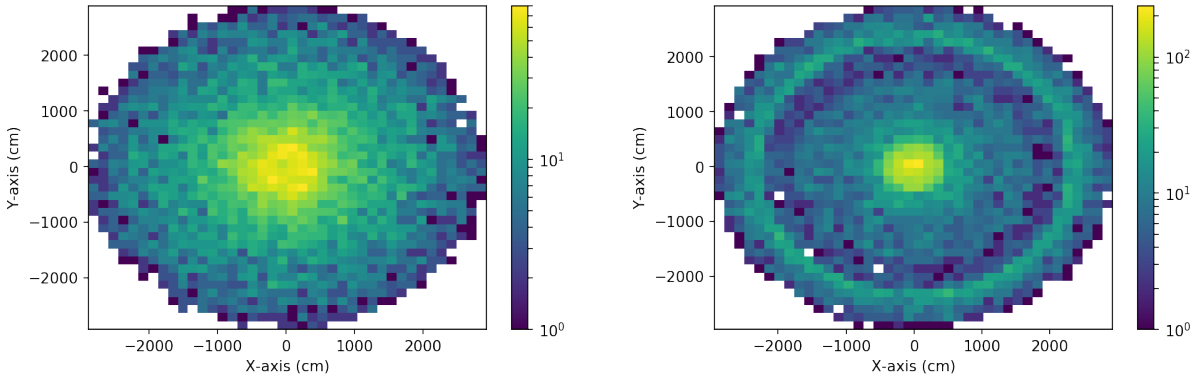

Figure 9: X-Y projection distribution of pion/kaon positions after propagation without magnetic field [left] and with magnetic field [right].

positive charged particles are focused along the beam axis and all negative charged particles are deflected away from the beam axis (which denotes the ring structure in the plot). Therefore we can conclude that focusing the particles with horn magnets is in agreement with the expectation.

Our next step is to incorporate the decay of pions and kaons and simulate the neutrinos as their decay products. $\pi^{\pm}$ has mean lifetime $\tau = 26.033ns$ and $K^{\pm}$ has the mean lifetime $\tau = 12.380ns$. In general, particle with mean lifetime τ follows the exponential decay as,

$$\begin{aligned} \frac{dN}{dt} &= -\frac{N}{\tau} \\ N &= N_0 e^{-t/\tau}. \end{aligned} \tag{14}$$

where N_0 is the initial number of particles and N is the number of particles at given time t. One can show that the decay probability of a particle is,

$$P(t) = \frac{e^{-t/\tau}}{\tau}. \tag{15}$$

Taking P(t) as the probability distribution function (pdf) of the decay, one can evaluate the cumulative distribution function (cdf) as,

$$\begin{aligned} C &= \frac{1}{\tau}\int_0^t e^{-t'/\tau}dt' \\ t &= -\tau log(1-C). \end{aligned} \tag{16}$$

Here C follows the uniform distribution between 0 and 1. So in our simulation, we generate the random number in [0,1) and calculate the decay time according to the exponential decay for each particle. After determining the decay time of each particle we allow `odeint` to run only up to the decay time. Applying the decay, we get the X-Y projection distribution of pions and kaons shown in Fig. 10 (using the entire dataset). In the plot, we notice that the outer ring of negative particles disappears. The reason for disappearance of the outer ring is that, those diverging negative particles decay at different times based on the decay distribution. Therefore the axial symmetry we had before (in Fig. 9) due to the propagation of all particles for same time duration disappears, smearing the outer ring. The effect is also applied for the positive particles, however these particles are accumulated around a fixed point (rather than a ring), so it is not affected by smearing effect. From the angular distribution in Fig. 10, we see that the distribution of negative charged particles peak at $\sim 60^0$.

At the end of the particle propagation (where the particle decays), we simulate the 2-body decay kinematics as discussed in section 2. In the CM frame of pions and kaons, we randomly choose $(cos\theta_{CM}, \phi_{CM})$ for produced neutrinos from the uniform distributions in the

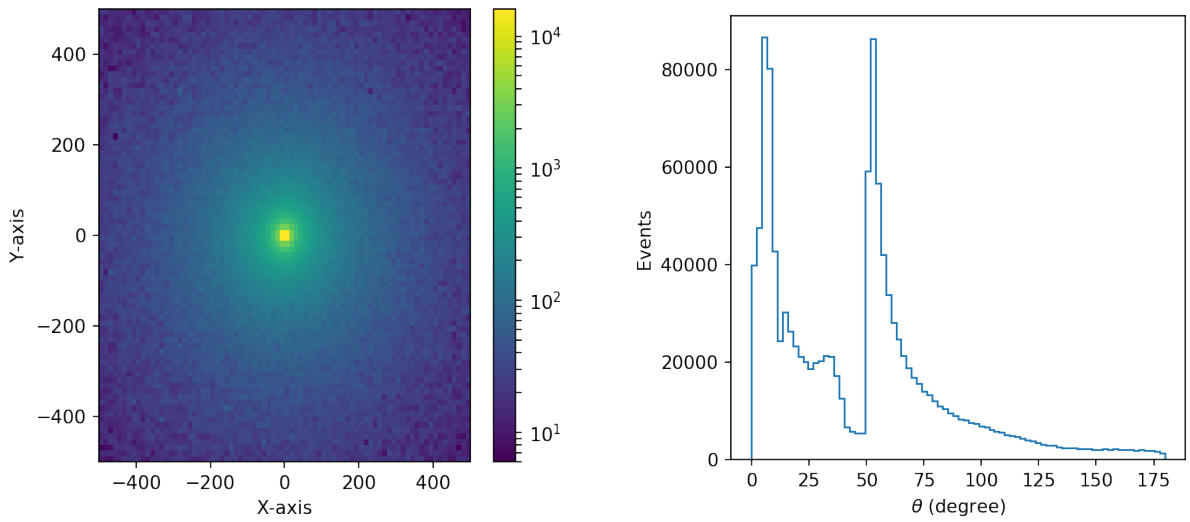

Figure 10: [Left]: X-Y projection distribution of pions/kaons with whole FLUKA dataset. [Right]: Angular distribution of pions/kaons after the propagation through magnetic fields.

range ($[-1, 1], [0, 2\pi]$). Then we apply the boost (function of pion/kaon energy) to get the neutrinos in the lab frame along the pion direction axis. However, note that the pions and kaons are not along the beam axis. Therefore to finally calculate neutrino energy and direction in the lab frame along the beam axis, we have applied Euler rotation on the pion-axis lab frame neutrinos (i.e. coordinate transformation by rotation). If the angles of pion/kaon in the beam axis coordinate denoted as (θ_p, ϕ_p) and the vector components of any quantity in pion-axis coordinate is denoted as (x_p, y_p, z_p). Applying coordination transformation using Euler rotation the vector components in beam axis coordinate (xx, yy, zz) is expressed as,

$$\begin{pmatrix} x' \\ y' \\ z' \end{pmatrix} = \begin{pmatrix} 1 & 0 & 0 \\ 0 & cos\theta_p & sin\theta_p \\ 0 & -sin\theta_p & cos\theta_p \end{pmatrix} \begin{pmatrix} x_p \\ y_p \\ z_p \end{pmatrix} \tag{17}$$

$$\begin{pmatrix} xx \\ yy \\ zz \end{pmatrix} = \begin{pmatrix} sin\phi_p & cos\phi_p & 0 \\ -cos\phi_p & sin\phi_p & 0 \\ 0 & 0 & 1 \end{pmatrix} \begin{pmatrix} x' \\ y' \\ z' \end{pmatrix}$$

In the first equation, rotation of angle θ_p is applied with respect to the X-axis of pion-axis coordinate. The components in the new rotated coordinate are then transformed by applying ϕ_p rotation with respect to Z-axis of the intermediate coordinate. After the coordinate transformation we have finally got the simulated neutrinos in our desired coordinate system.
To validate our decay kinematics simulation, we have reproduced Fig. 4 which shows the maximum neutrino energy as a function of pion energy at different angles. From Fig. 11 we see that the plot agrees with our expectation certifying the validation of our code.

With the production of neutrinos, we can now discuss the results by comparing with published results from T2K. Before discussing the results, we will now mention the limitations of our simulation in the next section.

4 Limtations on the simulation

The actual model of simulating T2K neutrino beam requires extensive work in detailed modeling of all possible physical effects of the accelerator system. In our toy simulation model, we have made as many simplified assumptions as possible to get the signature of important physics

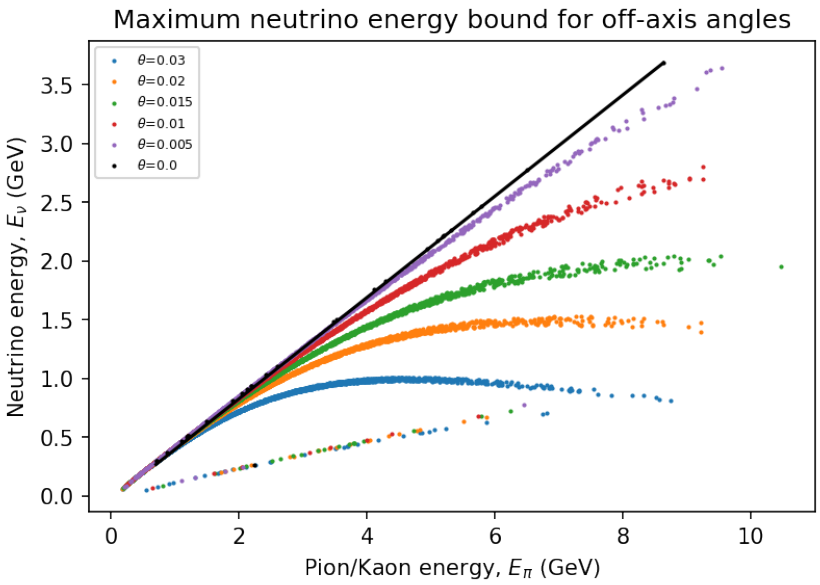

Figure 11: Simulated maximum neutrino energy as a function of pion/kaon energy at different θ.

effects. Following are the simplified assumptions we have made which can cause our results to be deviated from the actual simulation results:

- Our proton beam is mono-energetic peaked at 12GeV.
- We have simulated only 4×10^5 POT events compared to 3.3×10^{14} POT/pulse at T2K. So our statistics will be very low compared to the published results.
- There is no momentum spread in our proton beam. Each proton comes along the Z axis and interacts at the origin.
- We have assumed fixed 250kA current pulse (i.e. delta function) running through both magnets. However from Fig. 3 we see that the current pulse has a finite width.
- We have not considered the thickness of the inner and outer conductors of the magnets in our model. Finite thickness will cause edge effects in the magnetic field boundaries and also they will cause absorption and scattering of particles crossing through the conductor surfaces.
- Collision of particles with the conductor surfaces will increase the temperature (also apply mechanical stress on the surfaces) which in turn will affect the current flow. We have not considered such effects in our model.
- We have considered the medium of particle propagation to be perfect vacuum, i.e. the energy will be conserved during their propagation.
- Our model only consists of $\pi^{\pm}$, $K^{\pm}$ 2-body decays for the neutrino production. We have neglected other processes for muon neutrino production in this model.
- We have also ignored the background electron neutrinos that come from muon decay.

These are the most significant limitations in our model which can cause our results to be deviated from published result.

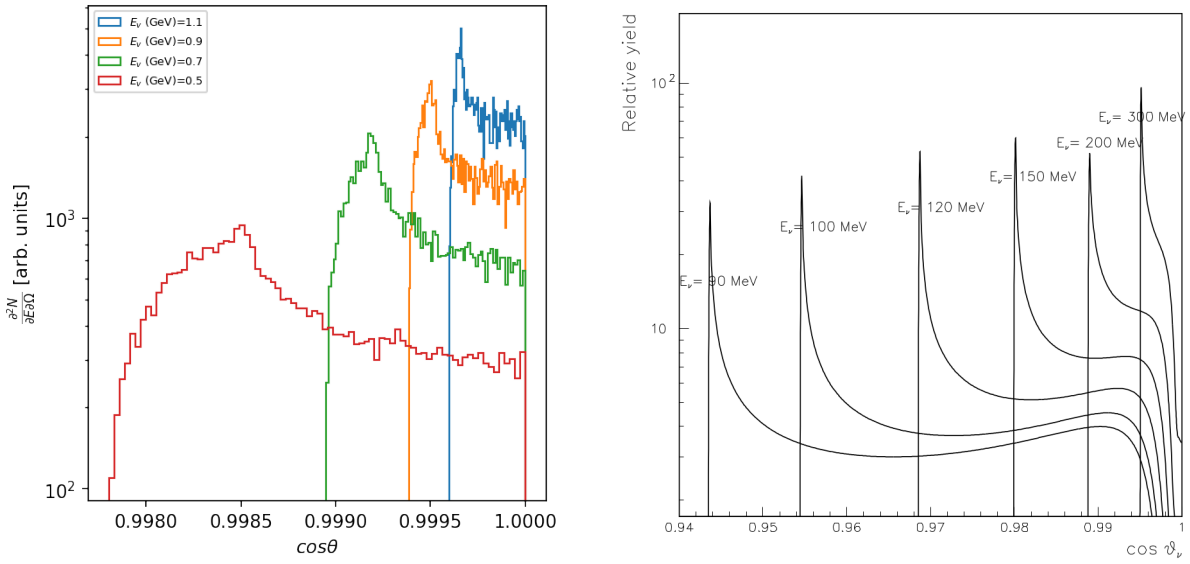

Figure 12: Neutrino beam spectrum as function of $\cos\theta$ at different neutrino energies in pion/kaon axis coordinate. [Left]:Simulation result, [Right]: from [7]

5 Results

After the end of simulation,, we have accessed the information of produced neutrinos and their parent pions/kaons. To study the properties of the neutrino beam, let us now consider respective pion-axis coordinates of each neutrinos. The neutrino spectrum as a function of $cos\theta$ at different energy E_ν in this coordinate system is shown in Fig. 12. The figure also shows the expected distribution and by comparing both distribution we see that our simulation result strongly agrees with the expectation. Note that the for lower energy, our statistics is too low to notice the shoulder effect close to the beam axis (i.e. $cos\theta \approx 1.$). For the neutrino energy $E_\nu = 1.1GeV$, small structure of the shoulder peak is noticeable.

Fig. 13 shows the neutrino flux spectrum as the function of E_ν at different off-axis angle (relative to pion direction axis). From the figure we notice that with increase of angle, peak energy of the spectrum shifts towards low energy scale. However at higher neutrino energy, we notice broad width of the distribution. The width decreases as we go higher in off-axis angle. Considering larger contribution from background along the beam axis, intensity of the beam and oscillation energy for the neutrinos, T2K has optimized its off-axis angle relative to the beam axis for SK detector to $2.5^0(\sim 0.044rad)$. In our spectrum plot we have included the spectrum at T2K off-axis angle (however this is relative to pion axis).

Finally Fig. 14 shows the neutrino beam spectrum as function of energy at different angle in the beam axis coordinate. First thing we notice from the plot is that our statistics is very low as we go higher in neutrino energy. From the expected plot, we notice that spectrum along the beam axis is highest in intensity, highest in peak energy and has the highest width. However in our plot, we do not see such behavior of the spectrum as go smaller in angle. The primary reason for this discrepancy is our very low statistics. If we look closely in Fig. 14, we notice that the peak energy for $\theta = 0.044rad$ is little shifted towards higher E_ν compared to the peak energy for $\theta = 0.09rad$. Also the width of the distribution increased for $\theta = 0.044rad$ which is consistent with our expectation. However, spectrum for $\theta = 0.01rad$ does not match our expectation as it falls with the increase of energy due to low statistics.

Therefore as our final result we report the neutrino beam spectrum for T2K experiment (i.e. $\theta = 0.044rad$) in Fig. 15 which has the similar distribution structure with the published neutrino flux spectrum (green line in the same figure). Our neutrino flux peaks at ~0.2 GeV

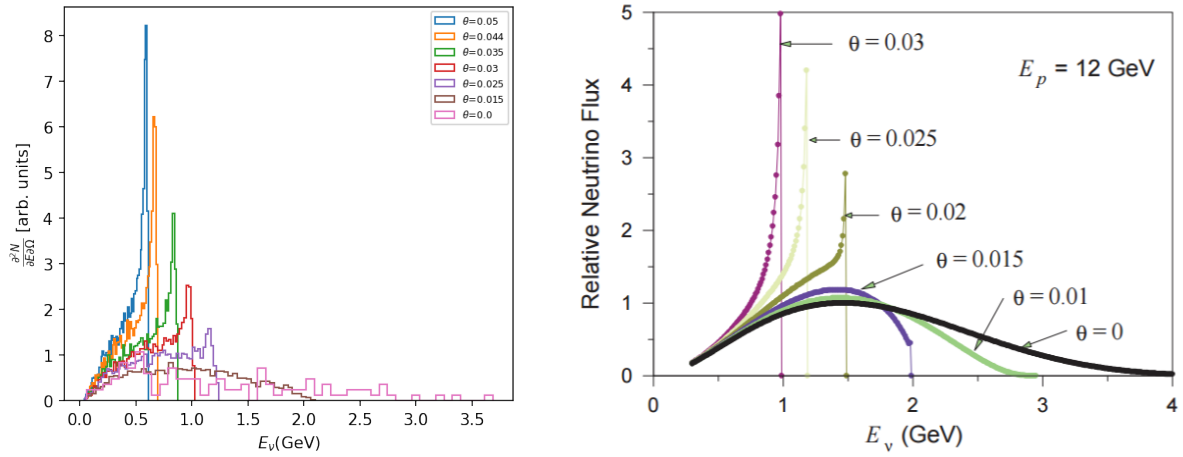

Figure 13: Neutrino beam spectrum as function of energy at different θ in pion/kaon axis coordinate. [Left]: Simulation, [Right]: from [9]

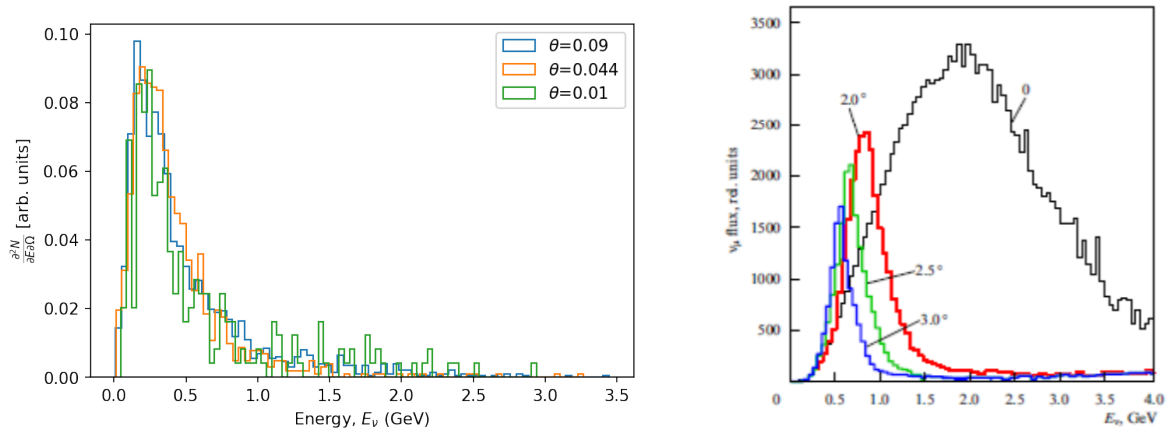

Figure 14: Neutrino beam spectrum as function of energy at different θ in beam axis coordinate. [Left]: Simulation, [Right]: from [10]

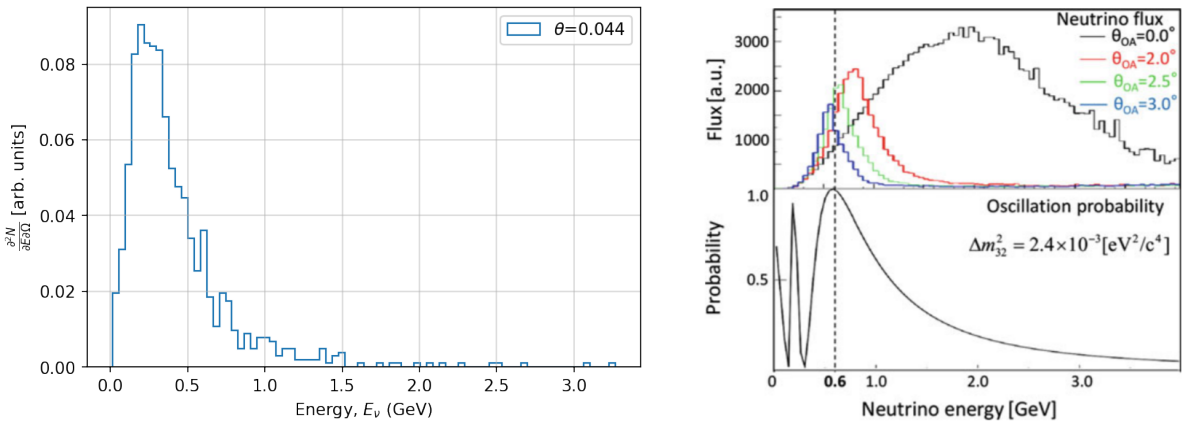

Figure 15: [Left]: Simulated neutrino flux at T2K off-axis angle, [Right]: spectrum from [1]

where as T2K spectrum peaks at 0.6 GeV at $\theta = 0.044rad$.

6 Conclusion

Fig. 15 shows the final result of our simulation which does not agree with the published result shown in the same figure. The primary reason for the discrepancy of the final result is our low statistics. However as we have discussed, intermediate results of our simulation agree with expectations through code validation process. Therefore we can conclude that our toy Monte Carlo model successfully investigates the principle physics processes involved in the simulation and generation of T2K neutrino beam.

References

[1] Ieki and Kei. *Observation of numu to nue Oscillation in the T2K Experiment*. Springer, 2016.

[2] Yu. G. Kudenko. Study of neutrino oscillations in long-baseline accelerator experiments. *Phys. Usp.*, 54(6):549–572, 2011.

[3] Sacha E. Kopp. Accelerator-based neutrino beams. *Phys. Rept.*, 439:101–159, 2007.

[4] S. van der Meer. A Directive Device for Charged Particles and Its use in an Enhanced Neutrino Beam. 1961.

[5] Y. Yamanoi, Y. Suzuki, E. Kusano, M. Minakawa, H. Nuomi, M. Ieiri, Y. Kato, K. H. Tanaka, M. Takasaki, M. Kohama, T. Maruyama, T. Inagaki, and K. Nishikawa. Large horn magnets at the kek neutrino beam line. ii. *IEEE Transactions on Applied Superconductivity*, 10(1):252–255, March 2000.

[6] Y. Yamanoi et al. Large horn magnets at the KEK neutrino beamline. In *15th International Conference on Magnet Technology (MT-15) Beijing, China, October 20-24, 1997*, 1997.

[7] Jean-Michel Levy. Kinematics of an off axis neutrino beam. 2010.

[8] A Ferrari, Paola R Sala, A Fasso, and Johannes Ranft. *FLUKA: A multi-particle transport code (program version 2005)*. CERN Yellow Reports: Monographs. CERN, Geneva, 2005.

[9] Kirk T McDonald. An Off-axis neutrino beam. 2001.

[10] D. P. Roy. Determination of the Third Neutrino-Mixing Angle. *J. Phys.*, G40:053001, 2013.

Appendices

FLUKA Input Code

```
* Input setting for pion production at proton aluminium collision
* ..+....1....+....2....+....3....+....4....+....5....+....6....+....7....+....8
TITLE
Pion production simulation in T2K detector
* ..+....1....+....2....+....3....+....4....+....5....+....6....+....7....+....8
BEAM             -12.0
PROTON
BEAMPOS      0.00E+00   0.00E+00   0.00E+00   0.00E+00   0.00E+00
*
GEOBEGIN
COMBNAME
    0    0          Cyllindrical itarget volume surounded by blackhole
* Body of blackbody
RPP body1       -200.   200.   -200.   200.   -200.   200.
* Body of aluminium cyllinder
RCC body2        0.0   0.0   0.0   0.0   0.0   65.0   1.0
END
* Blackhole region
regBH          5 +body1    -body2
* Target region
regTC          5 +body2
END
GEOEND
* End of detector geometry
* ..+....1....+....2....+....3....+....4....+....5....+....6....+....7....+....8
* Target aluminum material
ASSIGNMA     ALUMINUM      regTC
* External Blackhole material
ASSIGNMA     BLCKHOLE      regBH
* ..+....1....+....2....+....3....+....4....+....5....+....6....+....7....+....8
* Energy threshold for particle production and transport 100GeV
*EMF
EMF-OFF
*EMFCUT              1.          1.          1.         ICE
PROD-CUT
*EMFCUT         100000.     100000.         0.0      regIC1
*EMFCUT         100000.          0.          0.         ICE
ELPO-THR
*PAIRBREM           3.0     100000.     100000.         ICE
*PART-THR       100000.          1.0        62.0         1.0         0.0         0.0
*EMFCUT          1.0E-4       1.E-5         1.0         regIC1
PHYSICS            20.0        20.0        20.0        20.0        20.0        20.0PEATHRES
* score in each region energy deposition and stars produced by primaries
SCORE          ALL-PART
```

```
* Tracklength fluence inside the target, Upstream part and Downstream part
* Logarithmic energy intervals
* ..+....1....+....2....+....3....+....4....+....5....+....6....+....7....+....8
USERDUMP         100.                    0.0        1.0
 partlist
* ..+....1....+....2....+....3....+....4....+....5....+....6....+....7....+....8
USRTRACK          -1.  ALL-PART         -48.      regTC      1.E15       100. allflu
USRTRACK          50.      0.001
&
* Cartesian binning of the deposited energy inside the target
* ..+....1....+....2....+....3....+....4....+....5....+....6....+....7....+....8
USRBIN            10.     ENERGY         -41.     60000.     60000.     60000. Edeposit
USRBIN        -60000.    -60000.    -60000.        20.        20.        20. &
* ..+....1....+....2....+....3....+....4....+....5....+....6....+....7....+....8
RANDOMIZ           1.
* ..+....1....+....2....+....3....+....4....+....5....+....6....+....7....+....8
START         100000.
STOP
```